Heliyon

Received:
16 July 2018
Revised:
14 November 2018
Accepted:
20 December 2018

Cite as: Olaitan T. Ayegbusi, Oluwaseyi A. Ajagbe, Tosin O. Afowowe, Abideen T. Aransi, Babatunde A. Olusola, Ifeoluwa O. Awogbindin, Olukunle O. Ogunsemowo, Adedayo O. Faneye, Georgina N. Odaibo, David O. Olaleye. Virus genes and host correlates of pathology are markedly reduced during respiratory syncytial and influenza virus co-infection in BALB/c mice. Heliyon 5 (2019) e01094. doi: 10.1016/j.heliyon.2018.e01094

Virus genes and host correlates of pathology are markedly reduced during respiratory syncytial and influenza virus co-infection in BALB/c mice

Olaitan T. Ayegbusi [a,1], **Oluwaseyi A. Ajagbe** [a,1], **Tosin O. Afowowe** [a,1], **Abideen T. Aransi** [a,1], **Babatunde A. Olusola** [a], **Ifeoluwa O. Awogbindin** [b], **Olukunle O. Ogunsemowo** [a], **Adedayo O. Faneye** [a], **Georgina N. Odaibo** [a], **David O. Olaleye** [a,*]

[a] *Department of Virology, College of Medicine, University of Ibadan, Ibadan, Nigeria*

[b] *Department of Biochemistry, College of Medicine, University of Ibadan, Ibadan, Nigeria*

[*] Corresponding author.

E-mail address: davidoolaleye@gmail.com (D.O. Olaleye).

[1] These authors contributed equally.

Abstract

Globally, influenza A virus (IAV) and respiratory syncytial virus (RSV) infection remain very high. There is also a high burden of IAV and RSV co-infection in developing countries. To develop universally protective vaccines against these infections, it is imperative that viral genes and immune correlates of pathology are elucidated. As such, we profiled virus genes expressions, histopathology and immunological responses of BALB/c mice infected with RSV and/or IAV in this study.

RSV A2 and/or influenza A/H3N2/Perth/16/09 (Pr/H3N2) were induced over a seven-day period in BALB/c mice. Anaesthetized BALB/c mice (12−14 g) were divided into six groups (15−20 mice per group), inoculated with 32 μl each of $3LD_{50}$ Pr/H3N2 and/or 100 $TCID_{50}$ RSV. Two groups (R or I) received RSV or Pr/H3N2 intranasally. Prior infection with either RSV or Pr/H3N2 was followed

https://doi.org/10.1016/j.heliyon.2018.e01094

with a second challenge of the other virus 24 hours post inoculation in RI and IR groups. Another set was exposed to the two viruses simultaneously (I + R group) while the last group served as healthy controls. Five to seven mice per group were euthanized at days 2, 4 and 7. Lung and spleen organs were harvested for virus genes quantitation and immune cells phenotyping respectively.

I + R group showed progressive downregulation of RSV F, G, NS1 and NS2 genes. IAV PB2 and M genes had high fold increase on day 2 and 4 post infections. However, by day 7 post infection, M and PB2 fold increase was lower. Also, increased proportions of NKT and T cell subsets were observed throughout the period in I + R group. Conversely, I group was characterized by reduced NKT cell counts and enhanced CD8 T cells levels while R group only showed an increased proportion of CD8 T cells towards the peak of infection.

This study shows that RSV and IAV co-infection lead to reduced virulence and pathology compared to single infections. This information is very useful in combinatorial RSV/IAV vaccine design and development.

Keywords: Virology, Immunology

1. Introduction

Respiratory syncytial virus (RSV) is a major cause of lower respiratory tract infection in children globally (Lee et al., 2016). Most infants must have been infected by age two and more than a half of them are re-infected by age five years (Ogunsemowo et al., 2018; Eduardo et al., 2016). The virus also causes substantial morbidity and mortality in the elderly (With et al., 2015). On the other hand, influenza viruses especially influenza A (IAV) cause seasonal Flu that affects about 5−10% of the adult and 20−30% of the children population annually (Stevaert and Naesens, 2016). Concerns about sudden IAV pandemics also abound (Awogbindin et al., 2015).

In RSV and IAV single infections, pro inflammatory cytokines and viral genes involved in replication have been identified as correlates of disease severity. For IAV, NS1, NS2, M1 and PB2 genes have been shown to be associated with increased pathology (Chockalingam et al., 2016; Ka et al., 2014), while F and G genes have been implicated in the case of RSV (Baets et al., 2013; Lee et al., 2016; Oshansky et al., 2010). Moreover, Natural killer T (NKT) cells, antigen presenting cells as well as CD8 T lymphocytes have been associated with increased severity of symptoms although this have been shown to enhance viral clearance (Brand et al., 2013; Jozwik et al., 2015; Oshansky et al., 2010). Both IAV and RSV do not have effective vaccines. While there is no licensed vaccine against RSV, influenza virus vaccines are not universal and do not confer broad or lasting protection (Kratsch et al., 2016). Gaps in our understanding of the correlates of

https://doi.org/10.1016/j.heliyon.2018.e01094

protection and virulence during RSV and IAV infections are major barriers to development of effective vaccines.

Despite efforts to develop protective vaccines against RSV and IAV, studies on host-virus interactions in the context of RSV and IAV co-infections remain scanty (Stab et al., 2013; Turner et al., 2013; Walzl et al., 2000). Hence, there are no proofs of concept basis for these vaccines design. In effect, the viral as well as host immune correlates of protection and pathology during IAV and RSV co-infections are not fully known. Therefore, this study was carried out to elucidate the kinetics of viral genes and host's immune cells in the context of IAV/RSV single and co-infections in BALB/c mice. Concurrent and priori RSVA2 and IAV (H3N2) co-infections induced over a seven-day period were modeled in the study. H3N2 was chosen for this study because it is a well characterized strain used extensively for vaccine studies in research laboratories.

2. Materials and methods

2.1. Materials

Total RNA purification kit, SCRIPT cDNA Synthesis kit and qPCR GreenMaster with UNG/lowROX − blue dyed as well as primers were all obtained from Jena Bioscience (Jena Germany). Materials for tissue culture which include Gentamycin (10 mg/ml) antibiotics, Dulbecco's modified Eagle's medium and fetal bovine serum (FBS) were obtained from the WHO Polio Laboratory, Department of Virology, University of Ibadan. Hep-2 cell line used in the study was obtained from Infectious Disease Unit of Luxembourg Institute of Health. Fluorochrome-conjugated antibodies used for immunophenotyping analysis were produced by Biolegend, eBiosciences, BD Biosciences and Beckon Dickinson Co., and donated freely by Prof. Ross M. Kedl of the Department of Immunology and Microbiology, University of Colorado Denver, Aurora Colorado. 70 μM wire mesh MACS Smart Strainer was a product of Miltenyi Biotec GmbH (Bergisch Gladbach, Germany) while a hand-operated 7 ml Dounce Homogenizer used in the study was manufactured by Thomas Scientific, Swedesboro NJ, USA. Unless stated otherwise, other standard chemicals and reagents were obtained from Sigma-Aldrich (St. Louis, MO).

2.2. Sources and propagation of viruses

Characterized IAV isolate, A/H3N2/Perth/16/09 (Pr/H3N2), was obtained from the WHO Influenza Reference Centre, Medical Research Council, London. The isolate was first propagated in chorio-allantoic membrane of embryonated chicken egg and the harvested virus was adapted in BALB/c mice. The median lethal dose (LD_{50}) of the mouse-adapted IAV was determined using a 14-day procedure reported by Reed and Muench (1938). Influenza A virus matrix gene was amplified in both harvested

https://doi.org/10.1016/j.heliyon.2018.e01094

chorio-allantoic fluid and excised lung tissue by polymerase chain reaction (PCR) and detected by agarose gel electrophoresis.

Human RSV A2 (ATCC-1540) was obtained from the National Institute for Biological Standards and Control (NIBSC), Potters Bar, Hertfordshire, EN6 3QG, WHO International Laboratory for Biological Standard, UK Official Medicine Control Laboratory, and was propagated on Hep-2 cell line. The cells were grown in DMEM supplemented with 10% (w/v) FBS, 0.2% sodium biocarbonate and 1% Gibco antibiotic/antimycotic solution (containing 10,000 U/mL of penicillin, 10,000 μg/mL of streptomycin and 25 μg/mL of amphotericin B) and incubated at 37 °C until confluence. Stock virus was prepared and inoculated on semi-confluent monolayers of contaminant-free Hep-2 cells. Following the characteristic syncytia formation on the fifth day, the cells and medium from the monolayers were collected and clarified by centrifugation (10 mins at 1000 g/4 °C). The supernatant was aliquoted and stored at -80 °C until used. $TCID_{50}$ of the RSV A2 was also determined according to the method by Reed and Muench (1938).

2.3. Animals and innoculation

BALB/c mice (12−14 g) were obtained from the experimental animal breeding facility of the Faculty of Basic Medical Sciences, University of Ibadan, Nigeria. They were provided with quality animal chow (Ladokun Feeds Nig. Limited) ad libitum and were given free access to clean drinking water. Mice were acclimatized for a week before they were inoculated intranasally with 32 μl each of the RSV (100 $TCID_{50}$) and/or Pr/H3N2 (3 LD_{50}). Prior inoculation, mice were anesthetized with 10 mg/kg of ketamine intraperitoneally. The study was approved by the Animal Care and Use Research Ethics Committee (ACUREC) of the University of Ibadan and conducted in accordance to the international and institutional guidelines for the protection of animal welfare during experiments.

2.4. Experimental design

Six groups of BALB/c mice comprising 15−20 mice per group were used. A group constituted the uninfected control mice while two other groups served as RSV (R) and Pr/H3N2 (I) mono-infection groups. The remaining three experimental groups were challenged with both viruses but at different time points (Fig. 1A). While animals in the fourth group were inoculated first with Pr/H3N2 and then challenged with RSV 24 hours post Pr/H3N2 inoculation (IR), mice in the fifth group were pre-challenged with RSV 24 hours prior Pr/H3N2 inoculation (RI). Experimental animals in the last group received Pr/H3N2 and RSV (I + R) simultaneously in that order. Mice in the mono-infection groups were inoculated on the same day the experimental animals in the co-infected groups were receiving the second inoculation. The day second viral inoculation was given in co-infected groups was considered day 0.

https://doi.org/10.1016/j.heliyon.2018.e01094

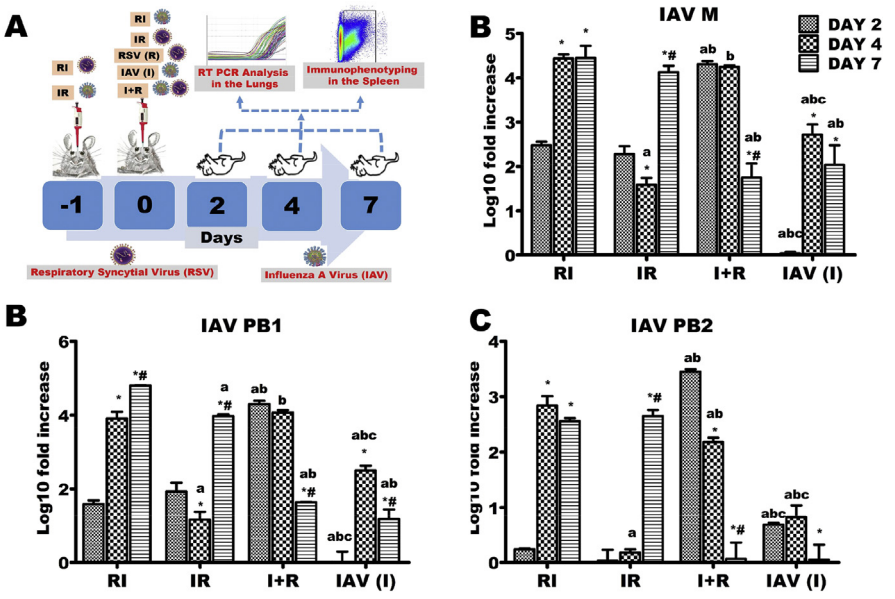

Fig. 1. Influenza A virus (IAV) M, PB1 and PB2 genes expressions across the experimental groups. Six groups of BALB/c mice were intranasally treated with 32 μl of normal saline (uninfected), RSV A2 (RSV(R)), Pr/H3N2 (IAV (I)) or co-treated simultaneously (I + R) or one after the other at 24 hours interval (IR and RI). (A) On days 2, 4 and 7, mRNA was extracted from lungs (n = 5) for real time PCR analysis of IAV genes. (B) mRNA expression level of M gene (C) mRNA expression level of PB1 (D) mRNA expression level of PB2. IAV M, PB1 and PB2 genes were expressed early on infection in I + R group and this was sustained up until the 4th day. CT values were normalized with GADPH, mRNA expression level was calculated using $2^{-\Delta\Delta CT}$ method and presented as Log10 fold increase relative to uninfected controls. mRNA expressions for IAV M, PB1 and PB2 were not detected in RSV (single virus) infected mice. * vs Day 2 and $^{\#}$ vs Day 4 for within group comparison while ^{a} vs RI, ^{b} vs IR and ^{c} vs I + R for comparing between groups of the same day ($p < 0.05$).

2.5. Sample processing

On days 2, 4 and 7 post infection, five mice were euthanized in each group. After euthanasia, whole lungs and spleen samples were excised and analyzed immediately. Lungs samples were processed for viral genes quantification by real time PCR (qPCR) while splenic tissues were processed for flow cytometry analysis. For histological analysis, a portion of the excised pulmonary tissues (n = 3) at each time point were stored in 10% neutral buffered formalin for at least a day. After fixation, they were sectioned, embedded in paraffin wax and processed further with hematoxylin and eosin stains to assess the severity of infections.

2.6. Quantitation of viral genes by qPCR

Expression levels of RSV M, G, F, NSI, NS2, Pr/H3N2 M, PB1, PB2 and glyceraldehyde-3-phosphate dehydrogenase (GAPDH) genes in control and infected mice were assessed using a two-step real time PCR protocol involving RNA extraction, cDNA synthesis and real time PCR amplification. The pulmonary tissue was

https://doi.org/10.1016/j.heliyon.2018.e01094

homogenized with lysis buffer in a hand-operated homogenizer. The homogenates were further processed for total RNA extraction using Total RNA purification kit (Jena Bioscience) according to manufacturer's instructions. Complementary DNA (cDNA) was synthesized from the extracted RNA using Jena Bioscience SCRIPT cDNA Synthesis Kit. The expression levels of the viral genes were quantified using SYBR-Green based real time PCR with Green Master mix and UNG/low ROX (Jena Bioscience) in Applied Biosystem 7500 Fast Real Time - PCR System. All procedures were carried out according to the manufacturer's instruction. For gene amplification, primers sequences and cycling conditions are presented in Table 1. Expressions were calculated as a ratio to the expression of the reference gene GAPDH relative to the control using the comparative Ct $2^{-\Delta\Delta C}$t method. Data were presented as log 10 of fold change. NS2 gene expression had incomplete data on day 2.

2.7. Flow cytometry

The spleen of each mouse was collected in FACS buffer and processed on ice to obtain splenic single-cell suspension used for flow cytometry analysis. Splenic tissues from experimental animals were tweezed in FACS buffer with frosted slides and passed through 50 μM filter into a 15 mL centrifuge tube containing cold FACS buffer. The filtrate was made up to a total volume of 10 mL with cold FACS buffer and centrifuged at 350 g for 5 mins at 4 °C. The pellet was washed two more times and re-suspended in 4 mL erythrocyte lysis buffer for 10 minutes after which the lysis buffer was washed off. The erythrocyte-free pellets were

Table 1. Primers sequence and cycling conditions.

Virus	Gene	Primer sequence	Cycling conditions	Product size
Influenza A(H3N2)	M	F:GACAAGACCAATCCTGTCACYTCTG R:AAGCGTCTACGCTGCAGTCC	950C-2 mins, 950C-15 secs, 600C-1 min, 45 cycles	97 bp
	PB1	F:CCCCTGAATCCATTTGTCAGCCATA R:TAGAGCGGTTCCTCTTGGGA	950C-30 secs, 550C-30 secs, 720C-30 secs, 40 cycles	142 bp
	PB2	F:ATTGCGGCCAGGAACATAGT R:CCAATTTGTGTGCTGTGGCA	950C-30 secs, 550C-30 secs, 720C-30 secs, 40 cycles	89 bp
RSV A2	M	F: GGCAAATATGGAAACATACGTGAA R:TCTTTTTCTAGGACATTGTAYTGAACAG	940C-2 mins, 940C-30 secs, 600C-1 min, 45 cycles	134 bp
	F	F:ATGAACAGTTTAACATTACCAAGT R:GTTTTGCCATAGCATGACAC	950C-2 mins, 950C-15 secs, 600C-1 min, 45 cycles	132 bp
	G	F:CGGCAAACCACAAAGTCACA R:TTCTTGATCTGGCTTGTTGCA	950C-2 mins, 940C-30 secs, 540C-30 secs, 720C-1 min, 720C-10 mins, 40 cycles	43 bp
	NS1	F:ATTTAACTCCCTTGGTTAGAG R:GTGTTAGTGACATTGATTTGC	950C-2 mins, 950C-30 secs, 530C-30 secs, 720C-30 secs, 40 cycles	482 bp
	NS2	F:TATGGCACTTTCCCTATGCCAA R:GGGTGTGTGCTTGGTAGGCT	95 °C-2 mins, 95 °C 30 secs, 58 °C-30 secs, 72 °C-30 secs, 40 cycles	

https://doi.org/10.1016/j.heliyon.2018.e01094

re-suspended in 1mL of FACS buffer and stained with 10 µl of trypan blue for cell counting. Cells were re-suspended to 2 × 10^6 cells/ml. 200 µl of cell suspension (i.e. 400,000 cells) were aliquoted into each Rohren tubes, washed and stained with 100 µl of pre-titrated antibody cocktail comprising antibodies in FACS buffer while 100 µl of FACS buffer was added to the unstained control. Cells were stained with antibodies from BD Biosciences (anti- NK1.1, FITC; anti-CD4, FITC; anti-CD11b, FITC; and anti- CD11c, PE), Biolegend (anti-CD3e, PE; anti-CD3e, PerCpCy5.5; and anti-CD8a, APC), eBiosciences (anti-CD25, PE). Suspensions were then incubated at 37 °C for 30 minutes and each tube was later made up to 1 ml with FACS buffer. The suspensions were then centrifuged at 3000 rpm for 3 minutes and fixed for 10 minutes in 1 ml fixing buffer and spun at 3000 rpm for 3 minutes. Cells were re-suspended in 600 µl FACS buffer for acquisition.

Cells were kept on ice during staining while stained cells were always protected from light. Samples were processed on a two colour Partec Cube 6 (Partec GmbH, Munster, Germany) to detect and quantify specific cells of interest. At least 100, 000 events were acquired. Analysis and determination of different subsets were done in FlowJo flow cytometry analysis software vX.0.7 (Tree star, Inc. Flowjo Africa Scheme). Gating of surface markers or compensation was determined using control samples and the unstained approaches. The gating strategies for the panels, as shown in Fig. 2, were as follows: Natural killer T cell, CD3+NK1.1+; cytotoxic T cells, CD3+CD8+; helper T cells CD3+CD4+; activated helper T cells CD3+CD4+CD25+; activated cytotoxic T cells, CD3+CD8+CD25+; and myeloid cells (e.g. monocytes, macrophages and plasmacytoid dendritic cells (pDC)), CD3-CD11b + CD11c- or CD3-CD11b-CD11c+. All immune cells except NKT cells had incomplete data for days 2 and 4. Data for CD11b, CD11c, CD4,

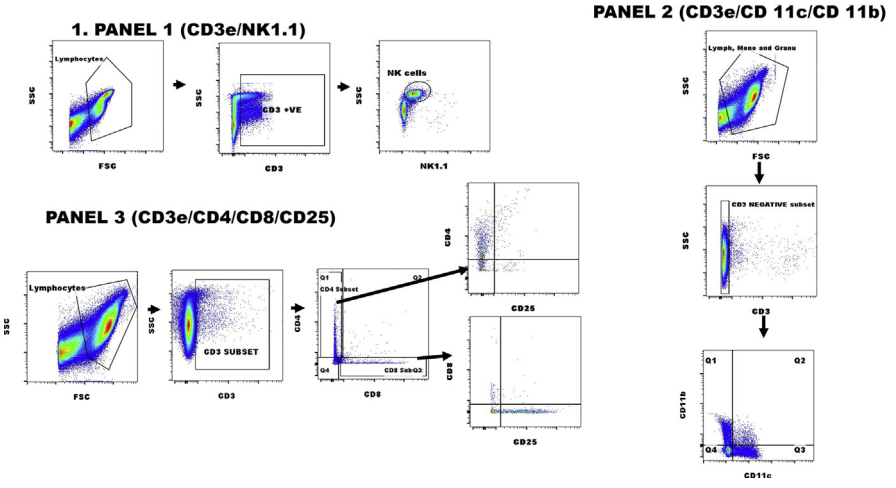

Fig. 2. Representative gating for flow cytometry analyses. Representative plots showing the gating strategies for quantitation of (PANEL 1) $NK1.1^+$ cells gated on $CD3^+$; (PANEL 2) $CD11b^+$ and/or $CD11c^+$ cells gated on $CD3^+$ and (PANEL 3) $CD25^+$ cells gated on $CD3^+CD4^+$ or $CD3CD8^+$.

https://doi.org/10.1016/j.heliyon.2018.e01094

CD4+CD25, CD8 and CD8+CD25 immune cells were unavailable for IR and RI as well as for IAV (I), RSV (R) and I + R on days 2 and 4.

2.8. Statistical analysis

Values of quantitative data were expressed as mean ± standard deviations. Comparison among groups was done by subjecting data obtained to the F-test (ANOVA) using SPSS statistical package for Windows, version 20.0 (SPSS Inc., Chicago, IL). Values were considered as statistically significant at p-value less than to 0.05, unless stated otherwise.

3. Results

3.1. Concurrent co-infection of BALB/c mice with RSV and IAV elicited early expression of IAV polymerases and matrix genes

Expression levels of polymerase PB1 and PB2 genes (components of IAV ribonucleoprotein; vRNP), as well as M gene (a peripheral protein under viral envelope that serves as a scaffold for vRNP) were assessed by qPCR. M, PB1 and PB2 genes were markedly upregulated at day 2 in I + R group when compared with other experimental groups (Fig. 1B−D). These levels decreased sharply through days 4−7. In contrast, expression levels of these three genes at day 7 were several folds higher than the values at day 2 in IR and RI groups. In same vein, PB2 was downregulated in I group by day 7 (Fig. 1D).

3.2. Concurrent IAV and RSV challenge represses the expression of RSV F, G and M genes

R, IR and RI groups had significant increases in F gene expressions from day 2−7 (Fig. 3A). However, reverse was the case in I + R group as there were markedly reduced levels of F gene expressions at days 2, 4 and 7 (Fig. 3A). R group had an increased M gene expression from day 2−7. A similar trend was observed in IR and RI groups, although rate of increase was highest at day 4 in these groups (Fig. 3B). A very limited upregulation of M gene was however observed in the I + R group (Fig. 3B).

When compared with R group, IR and RI groups had reduced expression levels of RSV G gene at all tested time-points Fig. 3C). RSV G gene was upregulated in R and I + R groups on day 2 of the experiment. While R group had a reduced expression of G gene at day 4 (which was similar to the level at day 7), expression levels of this gene in IR and RI groups reduced markedly from day 2 through day 7 after which it was upregulated (Fig. 3C).

https://doi.org/10.1016/j.heliyon.2018.e01094

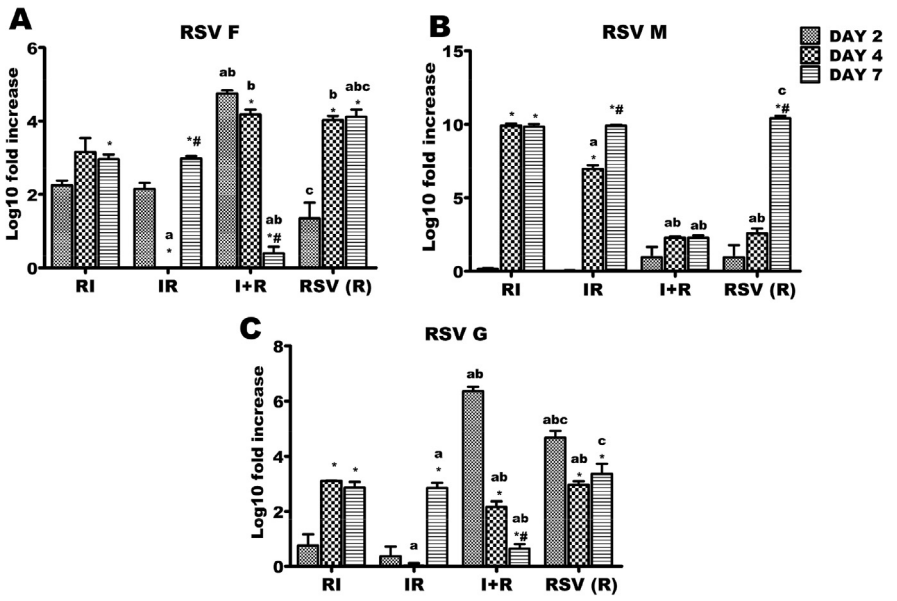

Fig. 3. Respiratory syncytial virus (RSV) F, G and M genes expressions across the experimental groups. Six groups of BALB/c mice were intranasally treated with 32 μl of normal saline (uninfected), RSV A2 (RSV(R)), Pr/H3N2 (IAV (I)) or co-treated simultaneously (I + R) or one after the other at 24 hours interval (IR and RI). On days 2, 4 and 7, mRNA was extracted from lungs (n = 5) for real time PCR analysis of RSV genes. (A) mRNA expression level of F gene (B) mRNA expression level of M (C) mRNA expression level of G. RSV F and G expression were markedly downregulated in I + R group by day 7 while RSV M expression was very low throughout the infection period in I + R group. CT values were normalized with GADPH, mRNA expression level was calculated using $2^{-\Delta\Delta CT}$ method and presented as Log10 fold increase relative to uninfected controls. mRNA expressions for RSV F, M and G were not detected in IAV (single virus) infected mice. * vs Day 2 and # vs Day 4 for within group comparison while [a] vs RI, [b] vs IR and [c] vs I + R for comparing between groups of the same day ($p < 0.05$).

3.3. Expression of RSV NS1 and NS2 was progressively downregulated in BALB/c mice concurrently infected with RSV and IAV

In RI and IR groups, there were upregulations of NS1 genes from day 2−7. This gene expression was progressively downregulated in R and I + R groups up until day 7 (Fig. 4A). For NS2 gene, downregulation from day 2 through 4 before an increase at day 7 was observed in the IR group; while I + R group had increase in this gene expression from day 4−7 (Fig. 4B).

3.4. Co-infection of BALB/c mice with RSV and IAV elicited a sustained reduction in the proportions of CD11b or CD11c myeloid cells

Reductions in the proportions of splenic CD3-CD11b + cells in the early stages of infection were prominent in all groups compared to the control group. However, towards the peak of infection at day 7, the reduction was only sustained in IR and RI

https://doi.org/10.1016/j.heliyon.2018.e01094

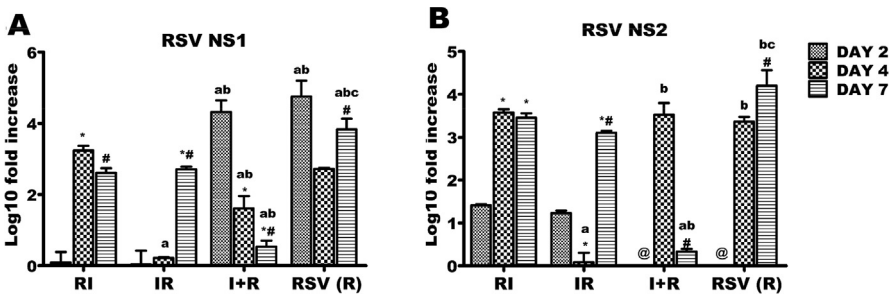

Fig. 4. Respiratory syncytial virus (RSV) NS1 and NS2 genes expressions across the experimental groups. Six groups of BALB/c mice were intranasally treated with 32 μl of normal saline (uninfected), RSV A2 (RSV(R)), Pr/H3N2 (IAV (I)) or co-treated simultaneously (I + R) or one after the other at 24 hours interval (IR and RI). On days 2, 4 and 7, mRNA was extracted from lungs (n = 5) for real time PCR analysis of RSV genes. (A) mRNA expression level of NS1 gene (B) mRNA expression level of NS2. RSV NS1 and NS2 expressions were downregulated by day 7 in I + R group. CT values were normalized with GADPH, mRNA expression level was calculated using $2^{-\Delta\Delta CT}$ method and presented as Log10 fold increase relative to uninfected controls. mRNA expressions for RSV NS1 and NS2 were not detected in IAV (single virus) infected mice. * vs Day 2 and # vs Day 4 for within group comparison while [a] vs RI, [b] vs IR and [c] vs I + R for comparing between groups of the same day ($p < 0.05$). [@] No data was available for I + R and RSV (R) on day 2.

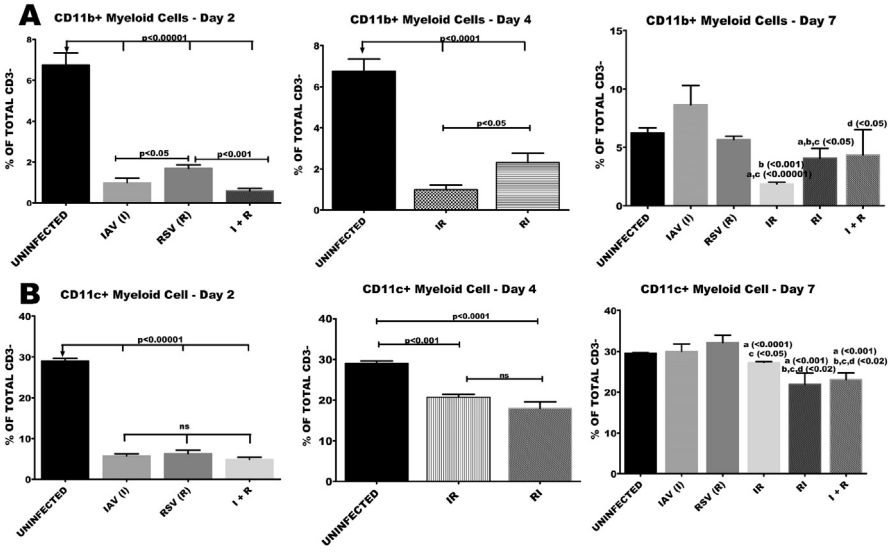

Fig. 5. Co-infection elicited reduction in the number of CD11b or CD11c myeloid cells. Six groups of BALB/c mice were intranasally treated with 32 μl of normal saline (uninfected), RSV A2 (RSV(R)), Pr/H3N2 (IAV (I)) or co-treated simultaneously (I + R) or one after the other at 24 hours interval (IR and RI). On days 2, 4 and 7 splenic cells (n = 5) were processed for flow cytometric analysis. to determine the frequency of NK1.1 gated on CD3 negative cells. (A) Proportion of CD11b myeloid cells, which was significantly low in the I + R group on day 2 was increased by day 7. (B) Proportions of CD11c myeloid cells were lower in I + R group compared to other groups on days 2 and 7. Unless indicated by lines, [a] vs uninfected, [b] vs IAV (I), [c] vs RSV (R), [d] vs IR, [e] vs RI. No data was available for IR and RI as well as for IAV (I), RSV(R) and I + R groups on day 2 and day 4 respectively.

https://doi.org/10.1016/j.heliyon.2018.e01094

groups. At this time, proportions of monocytes in I, R or I + R groups were statistically comparable with healthy controls (Fig. 5A). Splenic levels of myeloid cells expressing CD11c (pDC), characterized **by little or no expression of CD 11b** were also monitored. There was a marked reduction in the levels of these cells at days 2 and 4 in all the groups compared to healthy controls (Fig. 5B). By the seventh day, only RI and I + R groups had sustained reductions of pDCs levels. A mild but significant reduction was observed in the IR group when compared with R and healthy controls (Fig. 5B).

3.5. Concurrent infection of RSV and IAV induced high proportions of NKT cells during the early stages of co-infection

Throughout the study period, all groups had accumulations of natural killer T (NKT) cells when compared with healthy controls (Fig. 6). I + R group had a very early, enhanced and significant accumulation of natural killer T cells in the lymphoid organ and this was unabated till the animals were euthanized. Proportions of NK T cells were markedly high on day 7 across all groups except in I group in which there was a reduction from 21% of total CD3 on day 4−5% of total CD3 cells on day 7 (Fig. 6).

3.6. Concurrent infection of BALB/c mice with RSV and IAV resulted in early and sustained accumulation of T cell phenotypes

Accumulation of CD4 T cells was evident as early as day 2 in I + R group. By day 7, there were increased proportions of CD4T cells in I and I + R groups. There was a marked reduction in proportions of CD4 T cells in all the groups except R, I + R and IR at days 2 and 4 (Fig. 7A and B). Cytotoxic T cell counts were 15 folds higher in R group when compared with healthy controls (Fig. 8A and B). By day 7 a significant reduction in the proportion of cytotoxic lymphocytes in IR, RI and I + R groups was

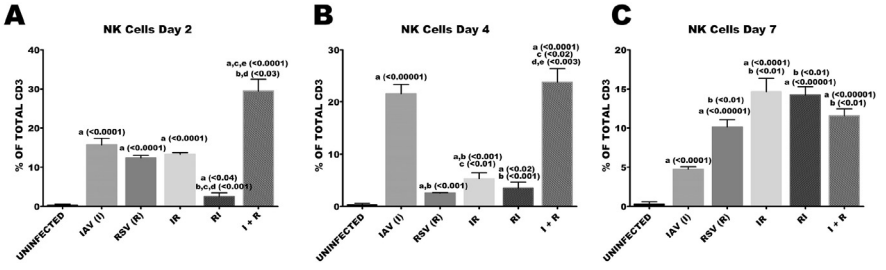

Fig. 6. Co-infection elicited high proportions of NKT cells. Six groups of BALB/c mice were intranasally treated with 32 μl of normal saline (uninfected), RSV A2 (RSV(R)), Pr/H3N2 (IAV (I)) or co-treated simultaneously (I + R) or one after the other at 24 hours interval (IR and RI). On days 2, 4 and 7 splenic cells (n = 5) were processed for flow cytometric analysis. (A) Proportions of NK1.1 cells gated on CD3 on day 2. (B) Frequency of NKT cells on day 4. (C) Frequency of NKT cells on day 7. Unless indicated by lines, [a] vs uninfected, [b] vs IAV (I), [c] vs RSV (R), [d] vs IR, [e] vs RI.

https://doi.org/10.1016/j.heliyon.2018.e01094

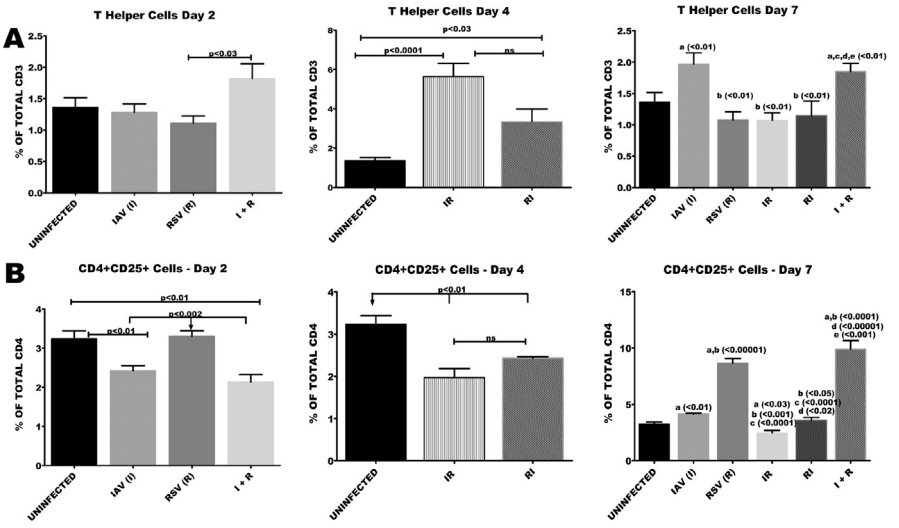

Fig. 7. Co-infection elicited very high numbers of CD4 and CD4+CD25 frequencies towards the later stages of infection. Six groups of BALB/c mice were intranasally treated with 32 μl of normal saline (uninfected), RSV A2 (RSV(R)), Pr/H3N2 (IAV (I)) or co-treated simultaneously (I + R) or one after the other at 24 hours interval (IR and RI). On days 2, 4 and 7 splenic cells (n = 5) were processed for flow cytometric analysis. (A) CD4 T cells proportions were high on days 2 and 7 in I + R group. (B) The frequency of CD4+CD25 T cells was highest in I + R on day 7. Unless indicated by lines, [a] vs uninfected, [b] vs IAV (I), [c] vs RSV (R), [d] vs IR, [e] vs RI. No data was available for IR and RI as well as for IAV (I), RSV(R) and I + R groups on day 2 and day 4 respectively.

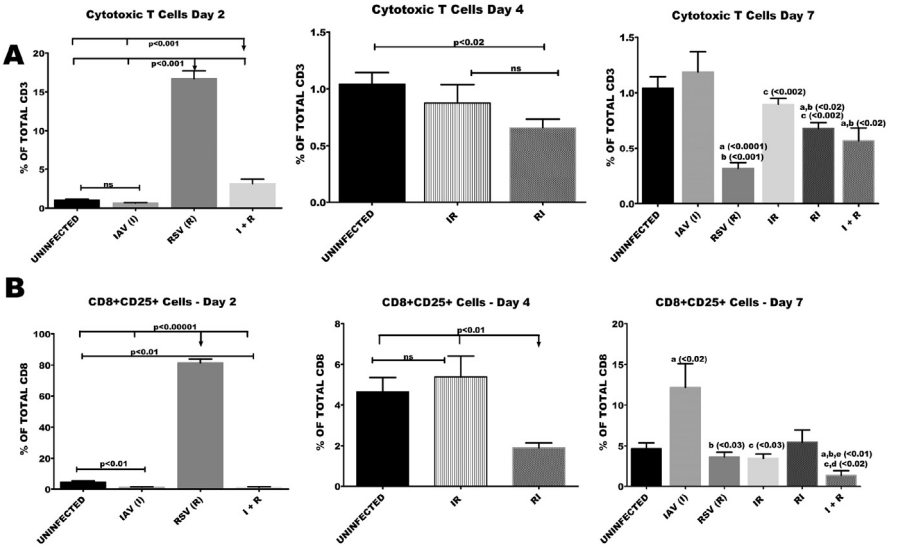

Fig. 8. Co-infection elicited very low numbers of CD8 and CD8+CD25 frequencies during the course of infection. Six groups of BALB/c mice were intranasally treated with 32 μl of normal saline (uninfected), RSV A2 (RSV(R)), Pr/H3N2 (IAV (I)) or co-treated simultaneously (I + R) or one after the other at 24 hours interval (IR and RI). On days 2, 4 and 7 splenic cells (n = 5) were processed for flow cytometric analysis. (A) CD8 T cells proportions were very low in I + R group compared to other groups. (B) The frequency of CD8+CD25 T cells was very low in I + R group compared to other groups. Unless indicated by lines, [a] vs uninfected, [b] vs IAV (I), [c] vs RSV (R), [d] vs IR, [e] vs RI. No data was available for IR and RI as well as for IAV (I), RSV(R) and I + R groups on day 2 and day 4 respectively.

https://doi.org/10.1016/j.heliyon.2018.e01094

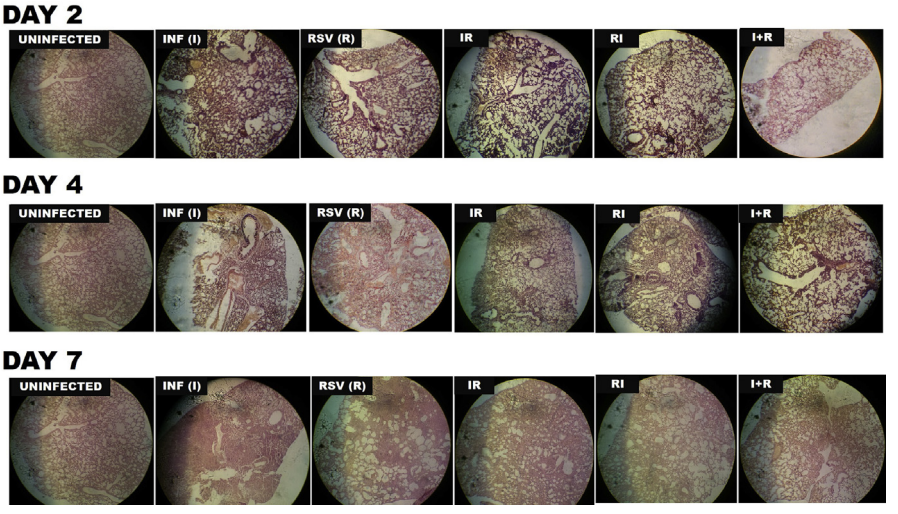

Fig. 9. Representative Hematoxylin and eosin (H&E)-stained sections of lungs from BALB/c mice mono- and/or co-infected with respiratory syncytial virus (RSV) A2 and influenza A/H3N2/Perth/16/09 virus (Pr/H3N2) Magnification is X20.

observed. This reduction was very prominent in I + R group. R group had the lowest count of cytotoxic T cells on day 7 (Fig. 8A).

3.7. Co-infected mice showed minimal pathology

Histopathology describes the extent and severity of infection in the lungs of mice infected with influenza virus and/or RSV over the time course of 7 days. As shown in Fig. 9 and described in Table 2, there was no obvious pathology in the lungs of uninfected mice as no inflammatory cell infiltrates were seen in the alveolar spaces. However, in R and I groups, there was a moderate to severe inflammation as the infection progressed from day 2−7 resulting in bronchitis, bronchiolitis, epithelial desquamation, emphysema and parenchyma thickening. IR, RI and I + R groups exhibited moderate pathology with the mildest being I + R group where mild alveolitis and diffuse interstitial thickening was observed. More pathological features and scores are described in Table 2.

4. Discussion

Few studies have attempted to determine host and viral markers of immunopathology in RSV and IAV co-infections. In this study, viral genes and host immune markers were compared among single IAV and RSV infections, priori and simultaneous RSV and IAV co-infections in BALB/c mice using qPCR, histopathology and flow cytometry techniques.

https://doi.org/10.1016/j.heliyon.2018.e01094

https://doi.org/10.1016/j.heliyon.2018.e01094

Table 2. Pulmonary pathological features of mice infected with RSV and/or IAV.

Group		Severity of inflammation		Infiltrated cells		Vascular changes		Pulmonary oedema	Alveolar and interstitial changes
		Description	Score (0−5)	Description	Score (1−10)	Description	Score (0−3)	Description	Description
Uninfected		Very mild or no inflammation	0	Very mild or no infiltrated cells	0	Normal vascular morphology	0	No pulmonary eodema	Normal parenchyma architecture was observed
INF (I)	Day 2	Mild inflammation in the interstitum	1	Mild infiltration dominated by neutrophils	3	Congested vasculature especially in the capillary	1	Moderate bronchiolar oedema	Moderate, diffuse and localized thickening of the respiratory bronchiolar epithelium. Desquamation of the walls delineating the bronchioles and alveolar duct
	Day 4	Widespread but diffuse inflammation with bronchial and epithelial proliferation	2	Severe and predominantly lymphocytic	7	Severe vascular congestion	3	Extensive eodema in the bronchiolar lumen and moderate interstitial oedema	Severe alveolar compression and loss of peri-bronchiolar wall
	Day 7	Widespread and severe inflammation affecting the interstitium, bronchi and alveoli	4	Predominantly lymphocytes and neutrophils	10	Moderate vascular congestion	2	No oedema	Severe parenchyma thickening that occluded almost all the parenchyma lumen
RSV (R)	Day 2	Diffused inflammation was noted	1	Mild infiltration dominated by neutrophils	4	Congested inter-alveoli capillary congestion	1	Oedema was conspicuously absent	Widespread thickening of the alveolar and bronchiolar walls.
	Day 4	Moderate to severe inflammation spanning wide area of the parenchyma.	3	High infiltration of inflammatory cells which are chiefly lymphocytes and neutrophils	6	Moderate to severe vascular congestion	2	Apparent oedematous alveoli which continued in the alveoli duct. Few oedematous respiratory bronchioles.	Severe alveolar compression widespread parenchyma thickening
	Day 7	Severe foci of inflammation affecting major portions of the interstitium and bronchi	4	Predominantly lymphocytes	7	Moderate to severe vascular congestion	2.5	Moderate oedema commonly seen in the alveolar duct	Formation of emphysema, severe thickening of interstitium and moderate alveolar compression

(*continued on next page*)

https://doi.org/10.1016/j.heliyon.2018.e01094

Table 2. (*Continued*)

Group		Severity of inflammation		Infiltrated cells		Vascular changes		Pulmonary oedema	Alveolar and interstitial changes
		Description	Score (0−5)	Description	Score (1−10)	Description	Score (0−3)	Description	Description
IR	Day 2	Moderate inflammation. No bronchial involvement	1	moderate lymphocytes and neutrophils	3.5	Moderate vascular congestion	2	Traces of Moderate eodema was seen in one of the representative photomicrographs. This was peculiar to certain alveolar duct loci	Mild alveolar compression with diffuse moderate interstitial thickening
	Day 4	Diffuse broncho-interstitial inflammation	2	Lymphocytic infiltration with traces of neutriphils	5	Mild to moderate congestion	1.5	Mild alveolar oedema	Moderate localized and diffused thickening with broncho-epithelial cells desquamating into the lumen
	Day 7	Acute and moderate broncho-interstitial pneumonia	3	Predominantly lymphocytes and neutrophils	6.5	Moderate to severe vascular congestion	2	Moderate oedema in the alveolar sac. The oedema also migrated to the lumen of the adjoining alveoli.	Severe, diffuse interstitial thickening with evidence of fibrosis. There is emphysema formation.
RI	Day 2	Moderate inflammation. No bronchial involvement	1	Mild cellular infiltration comprising both neutrophils and lymphocytes	2	Mild to moderate capillary congestion	1.5	Very mild oedema	Moderate and diffuse interstitial thickening. Loss of epithelial integrity of certain epithelial bronchioles
	Day 4	Acute and moderate inflammation with bronchial epithelial thickening	2	Predominantly lymphocytic	6.5	Mild to moderate congestion	1.5	Mild oedema that spans the longitude of the bronchiole	Mild to moderate diffuse interstitial thickening
	Day 7	Acute and moderate thickening inflammation. Bronchial thickening was evident and intrabronchiolar debris was noted	2	Predominantly lymphocytic infiltration with lymphocyte-neutrophil ratio of about 70−30.	7	Mild to moderate capillary congestion	1.5	Very mild oedema	Emphysema formation, compression of alveoli and interstitial thickening

(*continued on next page*)

Table 2. (*Continued*)

Group		Severity of inflammation		Infiltrated cells		Vascular changes		Pulmonary oedema	Alveolar and interstitial changes
		Description	Score (0−5)	Description	Score (1−10)	Description	Score (0−3)	Description	Description
I + R	Day 2	Mild inflammation. No bronchial involvement	1	Lymphocytes and neutrophils of almost equal proportion	4	mild to moderate congestion	1..5	Moderate interstitial oedema	Compression of alveoli, mild to thickening by cellular infiltration
	Day 4	Acute and diffuse broncho-interstitial inflammation. Mild thickening of bronchial epithelium which ran along the bronchiolar tree	1	Predominantly lymphocytes and neutrophils in 40−60 ratio	6	Moderate to severe vascular congestion	2	Moderate oedema in the alveolar sac.	Multifocal areas of intracellular thickening and moderate alveolar compression
	Day 7	Acute and moderate alveolitis	3	Predominantly lymphocytes and neutrophils in 50-50 ratio	7	Moderate vascular congestion	1.5	Oedema was evident in a single respiratory bronchiole. Generally, a mild oedema was seen in the pulmonary parenchyma	Mild and diffuse interstitial thickening

https://doi.org/10.1016/j.heliyon.2018.e01094

Our findings indicate that single RSV and IAV infections progressed from moderate to severe disease when compared to RSV and IAV co-infections in which mild and moderate pathology were observed over the course of the study. RSV A2 or Pr/H3N2 single infections replicated maximally in the infected mice, though it seemed RSV was more virulent as the genes were more preponderant than IAV genes throughout the study period. Although, caution must be exercised when inferring mouse model studies to humans especially in RSV and IAV infections, this study corroborates findings elsewhere that have described more severe infections during single RSV and IAV infections when compared with cases of viral co-infections (Diaz et al., 2015; Kuchar et al., 2015; Ljubin-sternak et al., 2016). Severe immunopathology and mortality caused by IAV infection has been widely attributed to sustained activation of innate immune responses that supposedly should elicit viral clearance but paradoxically contribute to pathology via a typically defined mechanism known as cytokine storm (Awogbindin et al., 2017; Gruta et al., 2007).

Co-infection of BALB/c mice with RSV and IAV showed interference in the expressions of viral genes and this was associated with protection. For instance, the observed marked attenuation of pathology in I + R group was partly due to early significant upregulation of the IAV polymerases PB1, PB2 and vRNP's scaffold M1 genes. While this group expressed these three genes very early in the infection and at magnitude 3 folds higher than their counterparts in I group. PB2, PB1 and M1 were upregulated progressively till day 7 in IR and RI groups in a pattern similar to I group.

In the same vein, expressions of RSV genes were markedly affected in the co-infection groups especially in I + R. There was a strong repression of RSV F, G, NS1 and NS2 genes in these groups. However, as it was noted for influenza A virus genes, all investigated RSV genes in I + R group showed a surge in the expression level on day 2 even though these would reduce dramatically through day 7. This may imply that efficient virion formation (M), successful spread and infection of new cells (F, G, NS1 and NS2) were negatively impacted in the I + R group (Stab et al., 2013; Walzl et al., 2000).

Though RSV G gene was downregulated across the days among all groups, there were very high expression of this gene during the early stages of infection in R and I + R groups. This is noteworthy because the viral protein of this gene is translated early because it is needed for attachment which has been shown to be an epitope for neutralizing antibodies (Bian et al., 2014; Park and Chang, 2012). Early expression of the genes in these groups should aid in the proper activation of the adaptive immunity through the Th2 pathway. Downregulation of these genes in is likely to hamper stimulation of G specific antibodies. The reduced genetic expressions of RSV F and G in the co-infected groups may reflect a greater, efficient and regulated $CD8^+$ T and natural killer T cells effector responses (Abdul-Careem et al., 2012;

https://doi.org/10.1016/j.heliyon.2018.e01094

Small et al., 2010; Espinoza et al., 2014; Vallbracht et al., 2006; Espinoza et al., 2014).

Interference with expression of viral markers of immunopathology especially those involved in replication, immune escape, viral protein trafficking and packaging are important factors to consider during antivirals and vaccines development. It is noteworthy that expression of the PB2 in concurrent RSV and influenza infection in BALB/c mice strongly correlated with stimulation of Natural Killer T (NKT) cells (Table 3). NKT cells stimulation leads to expression of interferons and stimulation of plasmacytoid DCs which are professional APCs that can properly lead to clearance of viruses during infection. Although, cytokines expression were not quantified during this study, positive correlation observed between NKT Cells and PB2 showed that this virus host interaction was critical for clearance during co-infection. Furthermore, NKT cells are known to activate $CD8^+$ T cells during RSV infection (Hussell and Openshaw, 1998; Li et al., 2012) as well as following influenza infections. The observed early and sustained accumulation of $CD8^+$ T cells in this study may be associated with indirect response of NKT cells (Hussell and Openshaw, 1998; Li et al., 2012; Farrag and Almajhdi, 2016). Findings from this study were limited by incomplete data for CD11b, CD11c, CD4, CD4+CD25, CD8 and CD8+CD25 cells on days 2 and 4 due to machine data storage error. However, this was compensated for by histopathology studies during this period.

Table 3. Association among RSV and IAV viral gene expression, NK cells and CD8 T cells.

Viral gene expression	Correlation with NK cells activation during course of infection				Correlation with CD8 T cells activation during course of infection		
	Early stages (2−4 days)	Late stages (4−7 days)	R^2 value for I + R	Groups	Early stages (2−4 days)	Late Stages late (4−7 days)	Groups
IAV M	Positive	Positive	0.92	RI, I + R	Negative	Negative	RI, I + R
IAV PB2	Positive	Positive	0.99	RI, I + R[a]	Negative	Negative	RI, I + R
IAV PB1	Negative	Negative	−0.95	IAV, IR, I + R, RI[b]			
RSV F	Positive	Positive	0.96	A2[c], I + R[d]			
RSV G	Positive		0.78	A2,I + R	Positive		A2[e], I + R
RSV M	Positive	Positive	0.54	A2, I + R[f], IR, RI	Negative	Negative	A2, I + R, IR, RI
RSV NS2	Negative		−1.0[g]	A2, I + R, IR, RI			
RSV NS1	Negative	Negative	−0.80	IR, RI			

[a] Correlation coefficient reached significance (0.04) in this group.
[b] Positive correlation was observed only in the early stages for this group.
[c] Highest in this group in the latter stages.
[d] Only in the early stages.
[e] Highest value observed in this group.
[f] Correlation was higher in the early stages than latter stages for this group.
[g] Value was for two time points.

https://doi.org/10.1016/j.heliyon.2018.e01094

Taken together, viral virulence markers, notably, IAV PB2, PB1, M1, RSV F and M genes, were consistently upregulated throughout the course of infection in single and priori infections while they were downregulated in concurrent infection. This may be the major reason for reduced disease severity observed in concurrent RSV and IAV infection. The mechanism may possibly revolve around two phenomena, namely, suppression of the RSV genes and the regulation of influenza A virus elicited NKT and CD8+ T cells immune responses. This may in turn limit prolonged tissue-damage. In conclusion, co-infection of RSV and IAV appears to generate robust, effective viral-host interaction. Evidence of mild protection in this group suggests that the response emanating from the co-infection group may be dual-protective. This finding is insightful for a combinatorial vaccine against RSV and/or influenza A virus infection.

Declarations

Author contribution statement

Olaitan T. Ayegbusi, Oluwaseyi A. Ajagbe, Tosin O. Afowowe, Abideen T. Aransi: Performed the experiments; Contributed reagents, materials, analysis tools or data.

Babatunde A. Olusola, Ifeoluwa O. Awogbindin, Olukunle O. Ogunsemowo, Adedayo O. Faneye: Conceived and designed the experiments; Performed the experiments; Analyzed and interpreted the data; Wrote the paper.

Georgina N. Odaibo, David O. Olaleye: Conceived and designed the experiments; Contributed reagents, materials, analysis tools or data; Wrote the paper.

Funding statement

This research did not receive any specific grant from funding agencies in the public, commercial, or not-for-profit sectors.

Competing interest statement

The authors declare no conflict of interest.

Additional information

No additional information is available for this paper.

Acknowledgements

The authors deeply appreciate Prof. Ross M. Kedl of the Department of Immunology and Microbiology, University of Colorado Denver, Aurora Colorado for the donation of Fluorochrome-conjugated antibodies used for immunophenotyping analysis in the study.

https://doi.org/10.1016/j.heliyon.2018.e01094

References

Abdul-Careem, M.F., Mian, M.F., Yue, G., Gillgrass, A., Chenoweth, M.J., Barra, N.G., Chew, M.V., Chan, T., Al-Garawi, A.A., Jordana, M., Ashkar, A.A., 2012. Critical role of natural killer cells in lung immunopathology during influenza infection in mice. J. Infect. Dis. 206, 167−177.

Awogbindin, I.O., Olaleye, D.O., Farombi, E.O., 2015. Kolaviron improves morbidity and suppresses mortality by mitigating oxido-inflammation in BALB/c mice infected with influenza virus. Viral Immunol. 28, 367−377.

Awogbindin, I.O., Olaleye, D.O., Farombi, E.O., 2017. Mechanistic perspective of the oxido- immunopathologic resolution property of kolaviron in mice influenza pneumonitis. APMIS 125 (3), 184−196.

Baets, S. De, Schepens, B., Sedeyn, K., Schotsaert, M., Roose, K., Bogaert, P., Fiers, W., 2013. Recombinant influenza virus carrying the respiratory syncytial virus (RSV) F 85-93 CTL epitope reduces RSV replication in mice, 87, 3314−3323.

Bian, C., Liu, S., Liu, N., Zhang, G., Xing, L., Song, Y., Duan, Y., Gu, H., Zhou, Y., Zhang, P., Li, Z., Zhang, K., Wang, Z., Zhang, S., Wang, X., Yang, P., 2014. Influenza virus vaccine expressing fusion and attachment protein epitopes of respiratory syncytial virus induces protective antibodies in BALB/c mice. Antiviral Res. 104, 110−117.

Brand, H.K., Ferwerda, G., Preijers, F., Groot, R. De, Neeleman, C., Staal, F.J.T., Warris, A., Hermans, P.W.M., 2013. CD4+ T-cell counts and interleukin-8 and CCL-5 plasma concentrations discriminate disease severity in children with RSV infection. Pediatr. Res. 73, 187−193.

Chockalingam, A.K., Hamed, S., Goodwin, D.G., Rosenzweig, B.A., Pang, E., Ii, M.T.B., Patel, V., 2016. The effect of oseltamivir on the disease progression of lethal influenza A virus infection : plasma cytokine and miRNA responses in a mouse model. Dis. Markers.

Diaz, J., Morales-romero, J., Pérez-gil, G., Bedolla-barajas, M., Delgado-figueroa, N., García-román, R., López-lópez, O., Bañuelos, E., Rizada-antel, C., Zenteno-cuevas, R., Ramos-ligonio, Á., Sampieri, C.L., Orozco-alatorre, L.G., Mora, S.I., Montero, H., 2015. Viral coinfection in acute respiratory infection in Mexican children treated by the emergency service : a cross-sectional study. Ital. J. Pediatr. 1−8.

Eduardo, J., Paula, A., Souza, D. De, Nery, B., Fazolo, T., Quoos, F., Márcio, P., Tetelbom, R., 2016. Immunomodulator plasmid projected by systems biology as a candidate for the development of adjunctive therapy for respiratory syncytial virus infection. Med. Hypotheses 88, 86−90.

 https://doi.org/10.1016/j.heliyon.2018.e01094

Espinoza, J.A., Bohmwald, K., Céspedes, P.F., Riedel, C.A., Susan, M., Kalergis, A.M., Espinoza, J.A., Bohmwald, K., Céspedes, P.F., Riedel, C.A., Bueno, S.M., Kalergis, A.M., 2014. Modulation of host adaptive immunity by hRSV proteins. Virulence 5, 740−751.

Farrag, M.A., Almajhdi, F.N., 2016. Human respiratory syncytial virus . Viral Immunol. 29, 1−16.

Gruta, N.L. La, Kedzierska, K., Stambas, J., Doherty, P.C., 2007. A question of self-preservation: immunopathology in influenza virus infection. Immunol. Cell Biol. 85, 85−92.

Hussell, T., Openshaw, P.J., 1998. Intracellular IFN-gamma expression in natural killer cells precedes lung CD8þ T cell recruitment during respiratory syncytial virus infection. J. Gen. Virol. 79, 2593−2601.

Jozwik, A., Habibi, M.S., Paras, A., Zhu, J., Guvenel, A., Dhariwal, J., Almond, M., Wong, E.H.C., Sykes, A., Maybeno, M., Rosario, J. Del, Mallia, P., Sidney, J., Peters, B., Kon, O.M., Sette, A., Johnston, S.L., Openshaw, P.J., Chiu, C., 2015. RSV-specific airway resident memory CD8+ T cells and differential disease severity after experimental human infection. Nat. Commun. 6, 1−15.

Ka, C., Mok, P., Yeung, H., Lestra, M., Nicholls, M., Wai, C., Sia, F., 2014. Amino acid substitutions in polymerase basic protein 2 gene contribute to the pathogenicity of the novel a/H7N9 influenza virus. J. Virol. 88, 3568−3576.

Kratsch, C., Klingen, T.R., Mu, L., Mchardy, A.C., 2016. Determination of antigenicity-altering patches on the major surface protein of human influenza A/H3N2 viruses. Virus Evol. 2, 1−12.

Kuchar, E., Brydak, L., Wardyn, K., 2015. Incidence and clinical course of respiratory viral coinfections in children aged 0−59 months. Adv. Exp. Med. Biol.

Lee, Y., Hwang, H.S., Kim, M., Lee, Y., Cho, M., Kwon, Y., Lee, J.S., Plemper, R.K., Kang, S., 2016. Recombinant influenza virus carrying the conserved domain of respiratory syncytial virus (RSV) G protein confers protection against RSV without inflammatory disease. Virology. NIH Public Access 404−413.

Li, F., Zhu, H., Sun, R., et al., 2012. Natural killer cells are involved in acute lung immune injury caused by respiratory syncytial virus infection. J. Virol. 86, 2251−2258.

Ljubin-sternak, S.I., Marijan, T., T, I.I.T., Jasna, H.T., Gagro, A., Vraneš, J., 2016. Etiology and clinical characteristics of single and multiple respiratory virus infections diagnosed in Croatian children in two respiratory seasons. J. Pathog.

https://doi.org/10.1016/j.heliyon.2018.e01094

Ogunsemowo, O., Olaleye, D.O., Odaibo, G.N., 2018. Genetic diversity of human respiratory syncytial virus circulating among children in Ibadan, Nigeria. PLoS One 13 (1), e0191494.

Oshansky, C.M., Moore, E., Tripp, R.A., 2010. The host response and molecular pathogenesis associated with respiratory syncytial virus infection. Future Microbiol. NIH Public Access 279–297.

Park, M., Chang, J., 2012. Immunogenicity and protective efficacy of a dual subunit vaccine against respiratory syncytial virus and influenza virus. Immune Netw. 12, 261–268.

Reed, L.J., Muench, H., 1938. A simple method for estimating fifty percent endpoints. Am. J. Hyg. 27, 493–497.

Small, C.-L., Shaler, C.R., McCormick, S., Jeyanathan, M., Damjanovic, D., Brown, E.G., Arck, P., Jordana, M., Kaushic, C., Ashkar, A. a, Xing, Z., 2010. Influenza infection leads to increased susceptibility to subsequent bacterial superinfection by impairing NK cell responses in the lung. J. Immunol. 184, 2048–2056.

Stab, V., Nitsche, S., Niezold, T., Storcksdieck, M., Wiechers, A., Tippler, B., Hannaman, D., Ehrhardt, C., Klaus, U., Grunwald, T., Tenbusch, M., 2013. Protective efficacy and immunogenicity of a combinatory DNA vaccine against influenza a virus and the respiratory syncytial virus. PLoS One 8.

Stevaert, A., Naesens, L., 2016. The influenza virus polymerase complex: an update on its structure, functions, and significance for antiviral drug design. Med. Res. Rev. 36, 1127–1173.

Turner, T.M., Jones, L.P., Tompkins, S.M., Tripp, R.A., 2013. A novel influenza virus hemagglutinin-respiratory syncytial virus (RSV) fusion protein subunit vaccine against influenza and RSV. J. Virol. 87, 10792–10804.

Vallbracht, S., Unsold, H., Ehl, S., 2006. Functional impairment of cytotoxic T cells in the lung airways following respiratory virus infections. Eur. J. Immunol. 36, 1434–1442.

Walzl, B.G., Tafuro, S., Moss, P., Openshaw, P.J.M., Hussell, T., 2000. Influenza virus lung infection protects from respiratory syncytial virus – induced immunopathology. J. Exp. Med. 192, 1317–1326.

With, C., Respiratory, A., Wei, L., Liu, W., Zhang, X., Liu, E., Wo, Y., 2015. Detection of viral and bacterial pathogens in hospitalized children with acute respiratory illnesses, Chongqing, 2009–2013. Medicine (Baltimore) 94.

https://doi.org/10.1016/j.heliyon.2018.e01094